#6170

Numerical Simulation of Thermal Plumes in Rooms

A. Schaelin
Energy Systems Laboratory, ETH Zurich
CH-8092 Zurich

P. Kofoed
Sulzer Infra Group
CH-8401 Winterthur

SUMMARY

Thermal plumes have a great influence on the air flow pattern in rooms. While some experimental results are published and compared with analytical models for isothermal surroundings, only little is found on numerical simulation of such situations. Even less is found for thermal plumes in a ventilated confined space, which usually result in temperature stratification with a great influence on the evolution of velocity and temperature profiles.

In this work, a CFD (Computational Fluid Dynamics) code with the standard k-ε turbulence model has been applied to the simulation of thermal plumes in rooms with different temperature stratifications.

In the case of a fully developed self-similar flow, experimentally generated by a small circular heat source in the center of a room with no ventilation, the simulation results were compared with detailed measurements and analytical models. For this so-called point heat source the simulated peak values and radii of velocity and temperature profiles and the evolution of these quantities as functions of height show very good agreement with both the measurements and the anlytical models.

In the case of a flow from a heated vertical cylinder with the size and heat power of a sitting person, over 30 different situations with regard to ventilation parameters and resulting temperature stratification have been simulated. Due to the complexity of the flow, the experimental data were insufficient and a detailed comparison was not possible in some cases. At small temperature stratification levels, the experimental volume flow and the increased plume air volume flow with ventilation are also predicted by the simulation.

The overall agreement of the numerical results with the experimental measurements is very good and proves the value of numerical simulation for the ventilation engineer to model the effect of thermal plumes driving room air flow.

NUMERICAL SIMULATION OF THERMAL PLUMES IN ROOMS

A. Schaelin
Energy Systems Laboratory, ETH Zurich
CH-8092 Zurich

P. Kofoed
Sulzer Infra Group
CH-8401 Winterthur

1. INTRODUCTION

1.1. Thermal Plumes in Rooms

Room air flow is strongly influenced by thermal plumes caused by all types of heat sources present in rooms, e.g. heaters, computers, human bodies. Their influence on the flow is even more pronounced if the room ventilation is almost purely natural or only weakly forced as it is in the case of the displacement ventilation that has become popular in the last years. So, adequate models describing air flow with plumes are indispensable for the ventilation designers.

Figure 1a shows a typical schematic flow pattern in a room with a heat source and its associated plume that dominates the room air flow. The plume increases in width and velocity with height and entrains air from the sides. The flow behaviour of thermal plumes in conjunction with a displacement ventilation system is even more complex. Only a few detailed experimental data are available and only little is known about the performance of numerical codes in predicting the air flow in such situations.

Thermal plumes in rooms with temperature stratification have been the subject of the work carried out by Kofoed and Nielsen (1990). They investigated in detail plumes above a single heat source that was located in the centre of a test chamber, and compared the results with analytical predictions. Numerical simulation has been applied to turbulent buoyant plumes in free isothermal surroundings (open-air), and has been shown to agree well with analytical predictions for such plumes (Schaelin et al. 1992).

In this work, numerical simulation of air flow has been applied to the experimental situations of Kofoed and Nielsen (1990). The numerical results are compared with the measurements and analytical predictions.

1.2. Analytical Laws for Plumes

Figure 1b shows a plume in some more details. The buoyancy-driven air becomes turbulent after a while. For a small source the plume velocity and temperature profiles are axisymmetric and are characterized by the maximum values of velocity v and excess temperature ΔT and the profile widths. For the profile widths, the radii r_v and r_T are taken where the values v or ΔT drop to 1/e of its peak values, as shown in Figure 1b.

Turbulent buoyant axisymmetric plumes have been investigated for about 50 years already. For plumes in a uniform environment Schmidt (1941) derived for a point heat source following power law dependencies as functions of height z for peak velocity v, peak temperature ΔT, and plume width r_v:

$$v \sim z^{-1/3} \tag{1}$$

$$\Delta T \sim z^{-5/3} \tag{2}$$

$$r_v \sim z \tag{3}$$

The similarity hypothesis states that the velocity and temperature profiles are self-similar. Popiolek (1981) approximates the profiles by Gaussian functions

$$v(r,z) = f(z) \exp\left(-m\,(r/z)^2\right) \tag{4}$$

$$\Delta T(r,z) = g(z) \exp\left(-p\,(r/z)^2\right) \tag{5}$$

and derives following expressions

$$v = 0.023 \left\{ \frac{m^2}{p} + m \right\}^{1/3} Q_0^{1/3} z^{-1/3} \exp\left(-m\,(r/z)^2\right) \tag{6}$$

$$\Delta T = 0.011 \left\{ \frac{p\,(m+p)^2}{m} \right\}^{1/3} Q_0^{2/3} z^{-5/3} \exp\left(-p\,(r/z)^2\right) \tag{7}$$

For a good comparison of experimental and computational results, the following relations are helpful. Observing that the Gaussian velocity profile above a point source at a given height z is

$$v(r) = v_{max} \exp\left(-(r/r_v)^2\right) \tag{8}$$

it can be derived for the volume flux (Kofoed and Nielsen 1990)

$$\dot{V} = 2\pi \int_0^\infty v\, r\, dr = \pi\, v_{max}\, r_v^2 \tag{9}$$

2. EXPERIMENTAL SETUP

The experiments have been carried out in a full-scale test chamber described in detail by Kofoed (1991). Figure 3 gives an impression of the room with dimensions 8 m x 6 m x 4.6 m for length, width, and height, respectively. The room is equipped with a displacement ventilation system with two wall-mounted diffusors and to exhaust openings in the ceiling, so the room can be ventilated and different vertical temperature gradients created, if desired.

The plumes from two different heat sources placed in the exact centre of the room have been investigated. The large-scale instability of the plume is considered by using a multi-point measuring and data processing method. The method is called the extrapolation method and allows low measurement result scatter with regard to maximum velocity, temperature excess and plume integral parameter values, see Popiolek (1981) or Kofoed (1991). The temperature gradients outside the plume have also been recorded for the different experiments.

The first heat source is a steel tube, height 150 mm and diameter 50 mm, with a hot wire inside. For the measurements the source is placed vertically in a block of mineral wool (see Figure 2a). Source and mineral wool are raised 100 mm above the floor and the air sucked through the source from below.

The flow from the tube serves for the experimental verification of the point heat source model in a uniform environment. A fully developped flow with a zone of nearly complete similarity is obtained in the case of no mechanical ventilation of the room. The power supplied for the heat source is 343 W, and the convective part around 220 W.

The second heat source is designed as similar in size and effect to a sitting human body. It consists of a homogeneously heated black cylinder 1 m high and 0.4 m in diameter (see Figure 2b). The heating power is 100 W with a convective heat transfer to the air of about 25 W, derived from the experimentally measured profiles and also confirmed by the estimated radiation transfer to the room surfaces. The surface temperature is about 32 °C.

With this heat source situations with and without ventilations have been investigated, but the interpretation of the results turned out to be much more difficult than with heat source 1 because no self-similar flow regime was developed.

3. NUMERICAL SIMULATION

3.1. Description of CFD code

For the calculation of the airflow field and temperature distribution, the conservation equations of mass, momentum, and energy are solved in three dimensions for steady situations. A computer code developed and described by Rosten and Spalding (1987) was used in conjunction with the standard k-ε turbulence model (Launder and Spalding 1974) to solve the conservation equations in finite-volume form for pressure, velocity components, energy $h = c_p T$ (c_p, constant heat capacity; T, temperature), turbulent energy k, and dissipation of turbulent energy ε.

The solution procedure uses an upwind-difference scheme and staggered grids for the velocity components as described by Patankar (1980). The calculation is done under the assumption of incompressibility with the Boussinesq approximation for the buoyancy force.

The simulations were done mostly on a workstation with actual 5 MFLOPs performance for the implemented CFD code. A 3-dimensional 42 x 36 x 26 = 39312 cells case needs about 1000 sweeps to converge in a time of 8 hours.

3.2. Overview of numerical cases considered

Numerical simulations have been applied to two different cases, each with one of the two heater types. The "point source" type cases are labeled "RV*n*" and the cases with the cylinder heat source "RVC*n*". All the geometrical bodies and surfaces have been represented by cartesian bodies. So the hollow cylinder in source 1 (diameter 5 cm) is represented by a square opening of 4 cm width in a solid cube 80 cm wide and 10 cm high and situated 15 cm above the floor (without feet), and the source 2 is a cylinder (diameter 40 cm) modelled by a square of 40 cm width.

For the heat transferred to the air the convective part of the experimental value was taken, i.e. about 220 W in the point source case and about 25 W in the cylinder source case.

Figure 3 shows the cartesian grid used for the RV cases with a total of 42*36*26 = 39'312 grid cells. The RVC grid is similar with 42*34*25 = 35'700 cells. Note please that the z-coordinate points upright in the flow direction of the plume, as opposed to the work done by Kofoed (1991) where the upright coordinate has been chosen as x. The planes for which temperature and velocity profiles are shown later are indicated as x=6 and x=21. The numbers 6 and 21 refer to the grid number.

The RV cases have been calculated without ventilation, and for the RVC cases situations with and without ventilation have been considered, as in the experi-

ments. In the experiments the temperature pofiles across the room height range from almost isothermal (0.05 K/m or less) to moderately stratified (0.3 K/m).

Numerically the boundary condition at the walls and at the floor and the ceiling had to be adjusted slightly in order to fit the experimental conditions inside the room far from the plume. Wall temperatures etc. are not known in detail in the experiment. At the walls and at the ceiling a certain small heat flux outwards was prescribed, and the floor was held at the average air temperature. In the ventilation cases the inlet temperature was unknown and slightly varied to study the influence on the room air flow, as described in detail in Section 4.2.

4. RESULTS AND DISCUSSION

4.1. Cases with point source

The main case, with nearly complete similarity, is discussed in great detail in the work done by Kofoed (1991) or Kofoed and Nielsen (1990). The data are contained on page 150 or in Table 1, respectively, but only in the first case the vertical temperature gradient is given in detail.

The best fit of the experimental data with the analytical Gaussian profiles was obtained with a convected heat transfer value of 220 W and Gaussian profile parameters m=110 and p=115. These values are average values over the self-similar regime of the experimental flow pattern. The same m and p values were applied in this work for the comparison of the numerically calculated profiles with the analytical Gaussian profiles of Equations 6 and 7.

Figure 4 shows the flow field and some temperature contour lines in two planes for Case RV8. The off-plume temperature profile for the midplane (x=21) is almost the same as for plane x=6. This feature is common to all the cases calculated. The same heating power (220 W) as in the "E4" experiment derived for the convective part was applied in this numerical case.

The plume in this case RV8 is now analyzed and discussed in detail. Figure 5 shows the evolution of velocity and temperature peak as functions of the height z. In the range between 2 m and 3.5 m – which is the fully turbulent and self-similar range – the agreement with the experimental values are excellent (for the temperature even from 1.5 m on). A similar agreement holds for the analytical profiles after Equations 6 and 7 for the parameter values m=110 and p=115. For z > 3.5 m the numerical peak values drop down because of the stagnation effect of the ceiling, but no experimental values are available. The excellent fit with the parameters m=110 and p=115 means also that the entrainment factor is the same as in the measurement (Popiolek 1981, Kofoed and Nielsen 1990).

Figure 6 shows the velocity and temperature profiles across the plume in a typical (arbitrarily chosen) height of z = 2 m above the floor. The numerical profiles are compared with the Gaussian profiles after Equations 6 and 7. Again the agreement is very good even if the numerical profiles are a little bit narrower than the experimental ones. The numerical velocity and temperature profile widths at half maximum are narrower by 5% and 7.5%, respectively.

Figure 7 shows the evolution of the numerical velocity and temperature profile widths expressed in r_v and r_T (as in the work by Kofoed 1991) as functions of the height z. The velocity profile width agrees quite well with the experimental one from 1.2 m to 3.5 m, but is slightly less steep. The virtual cross section with the floor is at z_0 = - 0.5 m (as opposed to z_0 = - 0.25 m in the experiment). The numrical temperature profile width is considerably narrower by about 20% in the fully turbulent region.

Figure 8 shows the volume flux as calculated from Equation 9 for the numerical case. It is compared with the analytical expression

$$\dot{V} = 0.0051\, Q_0^{1/3} (z - z_0)^{5/3} \qquad (5)$$

derived from Equation 9 and 6 with parameter values m=110 and p=115. The numerical volume flux increase is slightly smaller because of the smaller velocity profile radius value that appears squared in Equation 9.

The overall agreement is very good with some deviations in the temperature profile width. What is not observed in the numerical results is a sharp distinction between transition and turbulent region. It looks as if the plume is already turbulent very shortly after the source as indicated by the fact that the numerical turbulence maximum is at about 1 m above the floor due to the high shear flow around the air outlet from the heat source. This is not very surprising because the k-ε model is known to be valid for fully turbulkent flow only. No physical model is implemented that describes the transition behaviour from laminar too turbulent. Wherever shear flow is found as around the plume core turbulence energy is calculated for fully turbulent flow.

Nevertheless the calculations turn out to be quite accurate at least for ventilation engineer purposes to model the effect of thermal plumes driving room air flow.

4.2. Cases with extended source

With the extended heat source the comparison of the numerical results and conclusions are considerably more difficult by following reasons: a) The plume profile near the source becomes non-Gaussian. b) The plume becomes non-axisymmetric. c) The whole plume becomes eventually tilted and even

partially disintegrated, depending on the parameters of the in-flow (as illustrated by Figure 13). So in these cases some conclusions will be more qualitative in nature.

Figure 9 shows the flow pattern of case RVC21 with the big cylindrical heat source of 22 W with no extra ventilation. Because the heat source is extended and also heated at the outside surfaces, the plume has in its first 30 cm the peak velocities in a circular region near the top edges and not in the middle as further above. If in addition ventilation is turned on the whole plume is slightly shifted in the inlet flow direction (not shown in a figure). The temperature stratification is only 0.05 K/m between a height of 2 and 4 m.

Figure 10 shows the flow pattern of case RVC92, which is the same as the previous case RVC21, with the ventilation turned on at a level of 0.7 ach and the air inlet temperature being the same as the average room temperature (20°C). The stratification is the same as in the previous case, and the plume flow pattern looks alike.

Figure 11a shows the evolution of velocity and temperature peak as functions of the height z for case RVC21. The profiles in the first m above the heat source are not Gaussian (they look more like a superposition of two Gaussian profiles immediately above the heat source), so the values cannot be compared to an simple function. At least the profile width approaches a linear function between a height of 3 m and 4 m. The situation is very similar for the case RVC92 with ventilation and therefore not shown here.

In the experimental work, the volume flux after Equation 9 has been investigated for the cases with extended heat source, and this evaluation is also shown for the numerical simulations. Fig. 11b shows now the volume flux for the two cases RVC21 and RVC92. For both cases, the volume flux is derived from an x- and a y-plane cut through the plume axis separately. The plume is not axisymmetric as in the point source cases, but has an elliptic cross-section, also in the case without ventilation, however more pronounced in the ventilation case. Between a height of 2.2 and 3.5 m the profiles are about Gaussian and the volume flux calculation is correct. The absolute level is the same (0.06 m^3/s at z=2 m and 0.10 m^3/s at z=3 m). The case with ventilation shows 5% more volume flux if one assumes an elliptical cross section and takes the geometrical average of the volume fluxes in the two perpendicular planes (i.e. square root of the product). The experimental shows about 10% more volume flux with ventilation, but the measurement spread is in the same order.

In the experimental work a third case was presented with a higher temperature stratification of 0.3 K/m. Such a level, homogeneously distributed across the height, could not be obtained in the numerical simulations. Over 30

different variations of floor, wall and ceiling temperature boundary conditions and of inlet temperature and mass flow have been tested, because all the mentioned temperature values have been unknown for the experimental cases. Following conclusions can be drawn from these parameter study:

a) The variation of +/- 1°C for the temperature or +/- 10 W per wall for the heat flux has been found to have no influence on the temperature stratification and on the flow pattern. The deviations have been assumed not to be higher in the experiment.

b) In order to yield a temperature stratification, the inlet air temperature has to be lower than the room average temperature. Homogeneous stratification levels of 0.3 K/m could not be reached by the described parameter variations. An air inlet temperature difference of -1 K or more is certainly realistic for the experimental case with a temperature stratification of 0.3 K/m because the air temperaure near the floor is 18.1°C and immediately at the floor 19.0°C (Kofoed 1990, page 170).

Figure 12 shows flow patterns and some temperature contour lines for a ventilation of 0.7 ach and varied inlet temperature difference between 0 and -2°C. Near the floor a cooler air layer develops with decreasing inlet air temperature. Figure 13 shows similar results for a temperature difference of -0.5°C and for ventilation rates from 0.7 to 4ach. Stratification is enhanced, but only at high ventilation levels. In the case of 4 ach, a stratification of 0.3 K/m is reached near the plume, but the plume is partially disintegrated. This figure shows also the tilting of the plume with incresing ventilation. However a quantitative comparison is not possible, because of the increasingly irregular shapes and because not enough experimental parameters are known.

The turbulence level in all the cases with cylindrical source is lower (turbulent kinetic energy is typically 10 times lower with the maximum located at the ceiling) than in the point source cases because the velocities are much lower near the cylindrical source. The plumes are still in the transition region and the self-similarity regime is probably not reached, but it cannot be seen clearly from the results because of non-Gaussian profiles. It was also derived for the experimental profile in the work of Kofoed and Nielsen (1990) that the plumes are still in the transition region.

5. CONCLUSIONS

Summarizing the results of the numerical simulations, following conclusions can be drawn:

- The overall agreement of the numerical results with the experimental measurements is very good with some excellent predictions.
- There are some deviations because the turbulence model is derived for fully turbulent flow and does not have the same accuracy for transition flow, and also because not enough experimental parameters are known for the setting of the numerical boundary conditions.
- For the point heat source case, the peak values of velocity and temperature profiles as a function of plume height agree almost perfectly with the analytical predictions derived from the self-similarity hypothesis. The experimental values are also well predicted in the turbulent region (from a height of 1.5 m above the heat source). In the experiment a transition region is observed below, near the heat source, which is not shown by the numerical simulations.
- Also profile widths for velocity and temperature and volume flow as a function of height are well predicted. The profile widths can be well fitted with the Gaussian profile parameters m=110 and p=115, which are derived from the measurements. It means that also the entrainment factor is predicted correctly, and the results can be considered reliable if the velocities of the plume and of the entrained air are correct.
- For the cases with extended heat source and at small temperature stratification the experimental results and the increased plume air volume flow with ventilation are also predicted by the simulation. A parameter variation shows the influence of air inlet temperature and air exchange rate on the temperature stratification in the room, but it cannot be compared in detail to the experimental situations because of insufficient data.

The overall agreement of the numerical results with the experimental measurements is very good and points out the practical value of numerical simulation for the ventilation engineer to model the effect of thermal plumes driving room air flow.

REFERENCES

Kofoed P.1991. Thermal Plumes in Ventilated Rooms. PhD Thesis. Dept. of Building Technology and Structural Engineering, Aalborg University, Aalborg, Denmark.

Kofoed, P., and P. V. Nielsen. 1990. Thermal plumes in ventilated rooms. Proceedings of ROOMVENT'90, Oslo, Norway.

Launder, B.E., and D.B. Spalding. 1974. The numerical computation of turbulent flows. Computer Methods in Appl. Mech. and Eng., 3: 269-289.

Patankar, S.V. 1980. Numerical heat transfer and fluid flow. , Hemisphere Publ. Corp, Washington, D.C.

Popiolek Z. 1981. Problems of testing and mathematical modeling of plumes above human body and other extensive heat sources. A4-series No. 54, Dept. of Heating and Ventilation, Royal Institute of Technology, Stockholm, Sweden.

Rosten, H.I., and D.B. Spalding. 1987. The PHOENICS reference manual, for Version 1.4, Report No. TR/200. London: CHAM Ltd.

Schmidt, W. 1941. Turbulente Ausbreitung eines Stromes erhitzter Luft. Z. angew. Math. Mech., 21(5): 264-278, and 21(6): 351-363.

Schaelin, A., van der Maas, J., and A. Moser. 1992. Simulation of Airflow through Large Openings in Buildings. ASHRAE Annual Meeting 1992, Baltimore, USA (to be published).

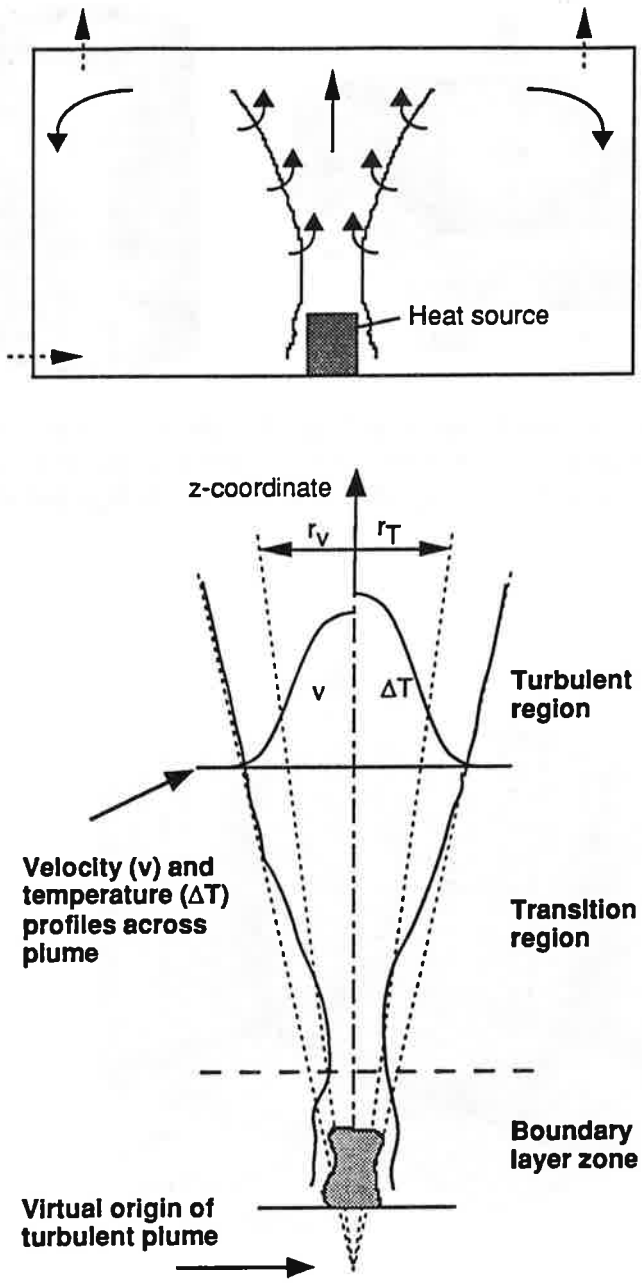

Figure 1: a) Flow in a room with heat source and plume above it. Dotted arrows indicate optional displacement ventilation. b) Thermal plume in detail with different regions. The plume profile parameters are shown in the schematic cross-sections.

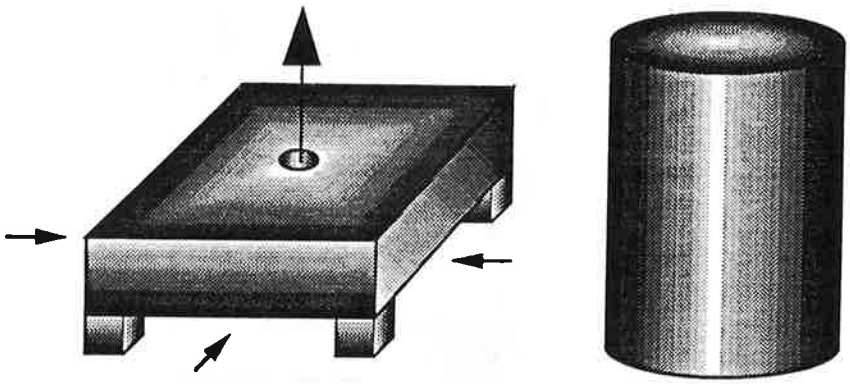

Figure 2: a) The "point source" is located in the hollow tube of 5 cm diameter isolated by a cube of 80 cm width and a height of 15 cm, 10 cm above the floor. b) Black cylinder heat source 1m high and 40 cm in diameter.

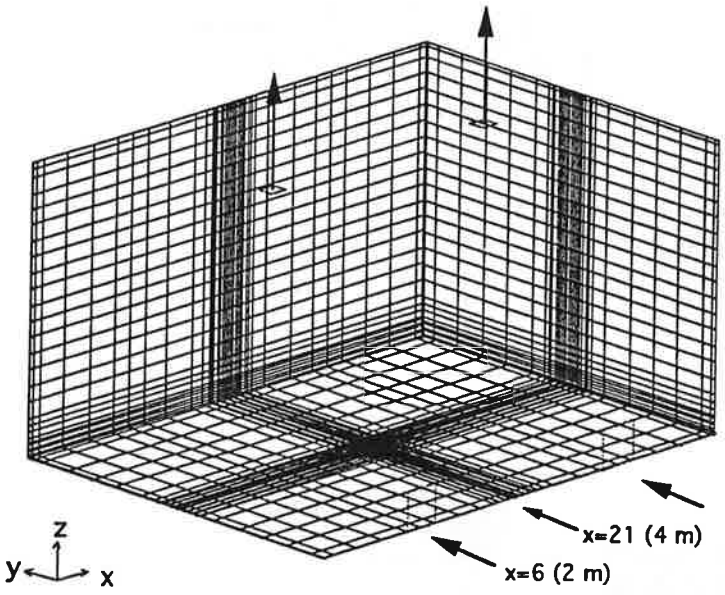

Figure 3: Grid for test chamber. Room size: xyz 8m*6m*4.6m, 42*36*26 cells, respectively. The heat sources are located in the exact room centre.

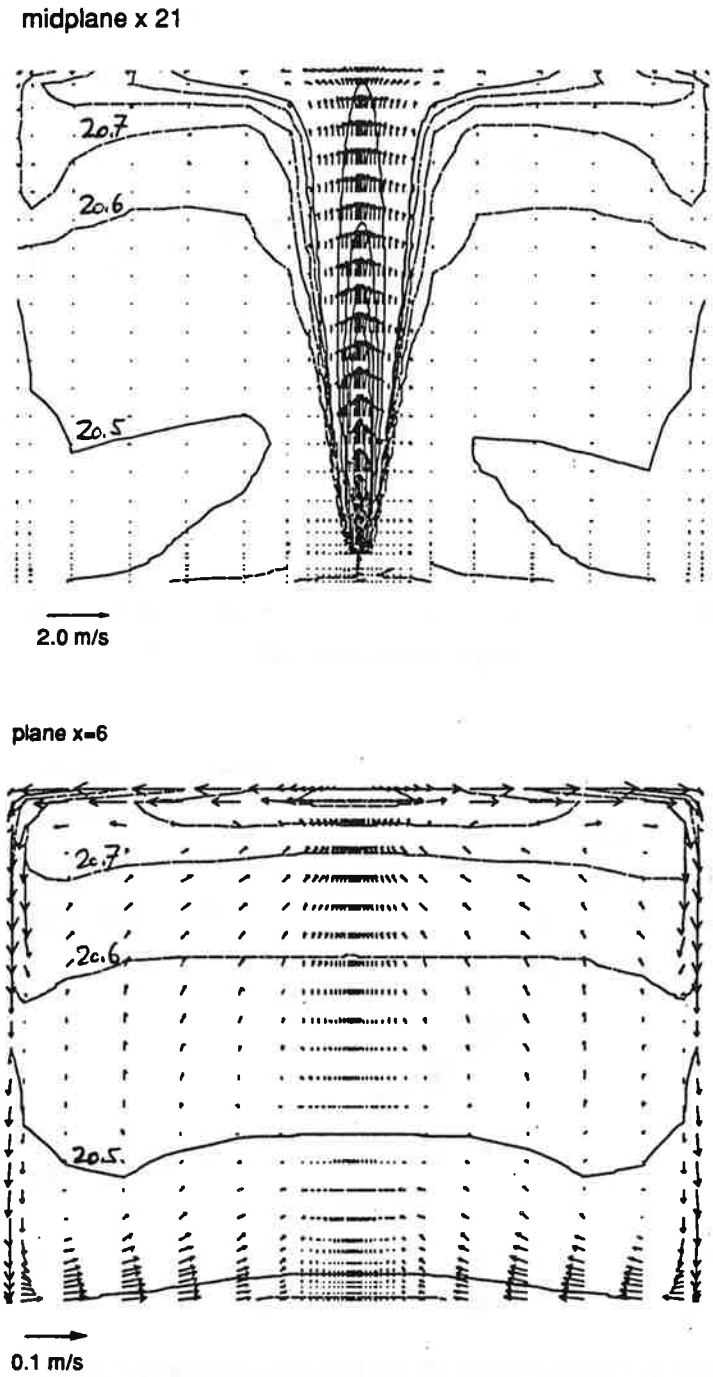

Figure 4: Case RV8. Flow pattern and temperature contour lines in two parallel planes (see Figure 3). a) Plane x = 21 (midplane). b) Plane x = 6.

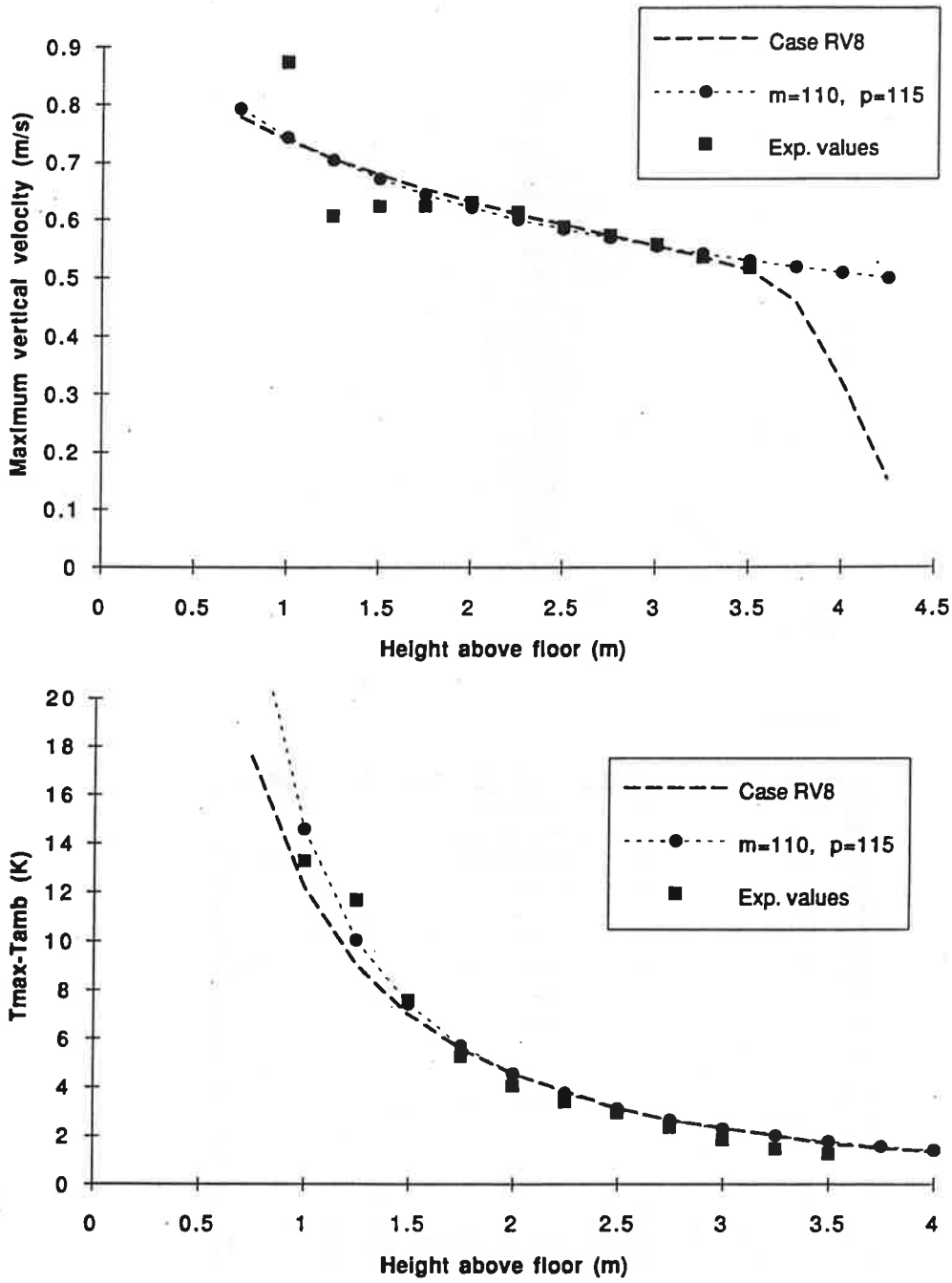

Figure 5: Case RV8. Comparison with experimental plume values as functions of height. a) Maximum of vertical velocity profile. b) Maximum of plume excess temperature.

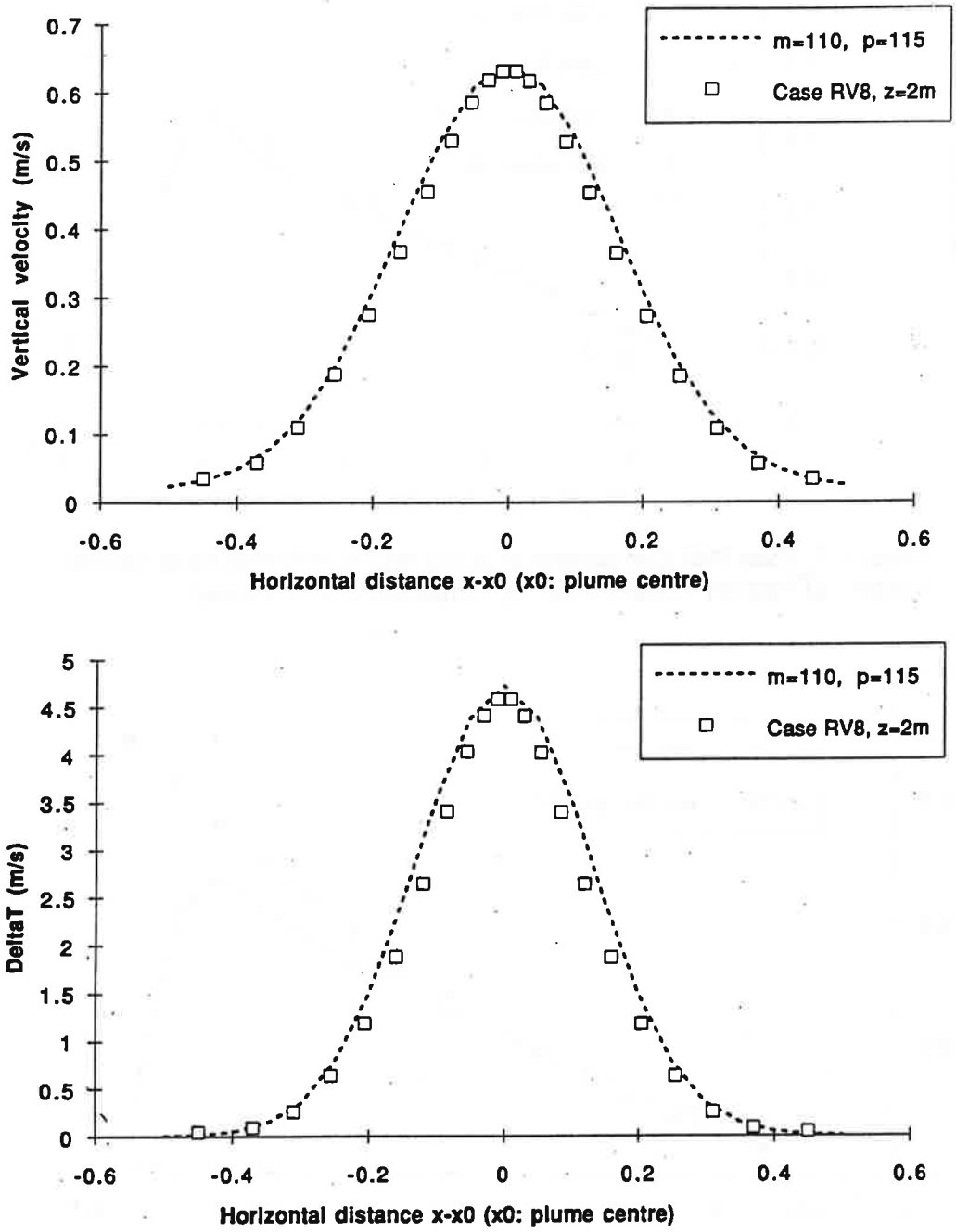

Figure 6: Case RV8. Comparison of plume profiles with experimentally derived Gaussian function. a) Velocity profile. b) Temperature profile.

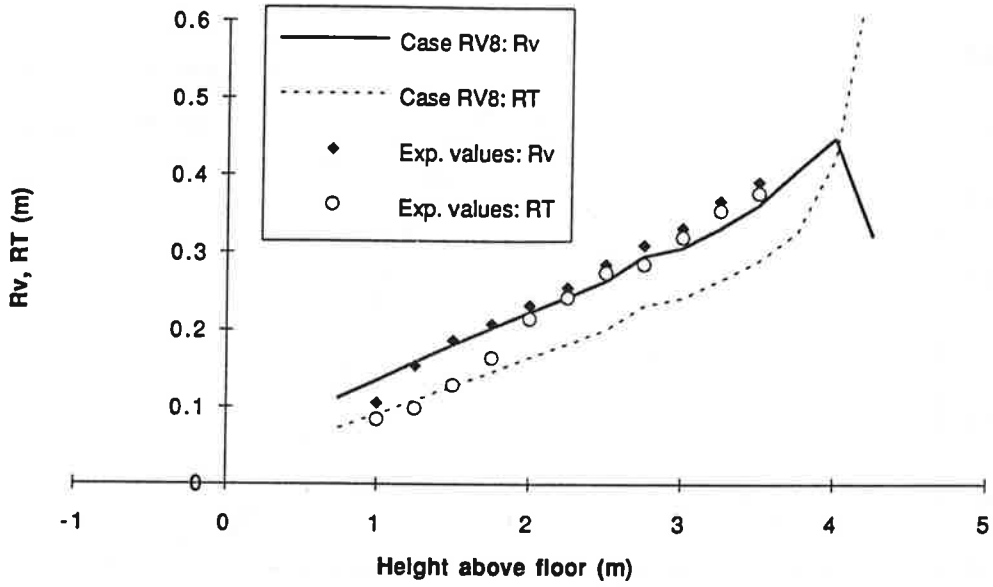

Figure 7: Case RV8. Comparison of plume profile radii with experimental values . a) Velocity profile radius. b) Temperature profile radius.

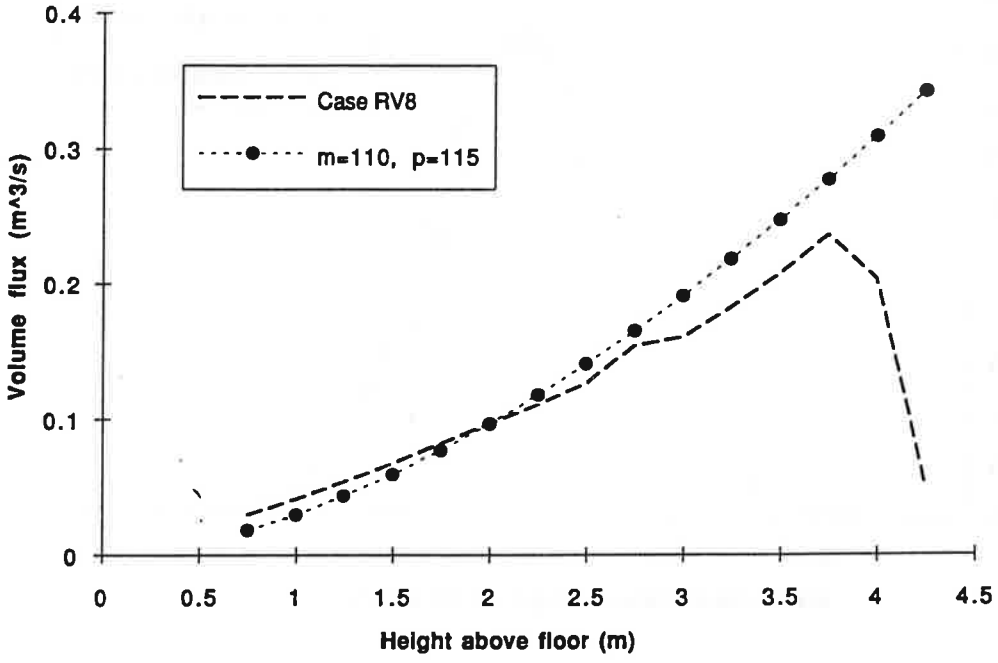

Figure 8: Case RV8. Comparison of volume flux with experimental values.

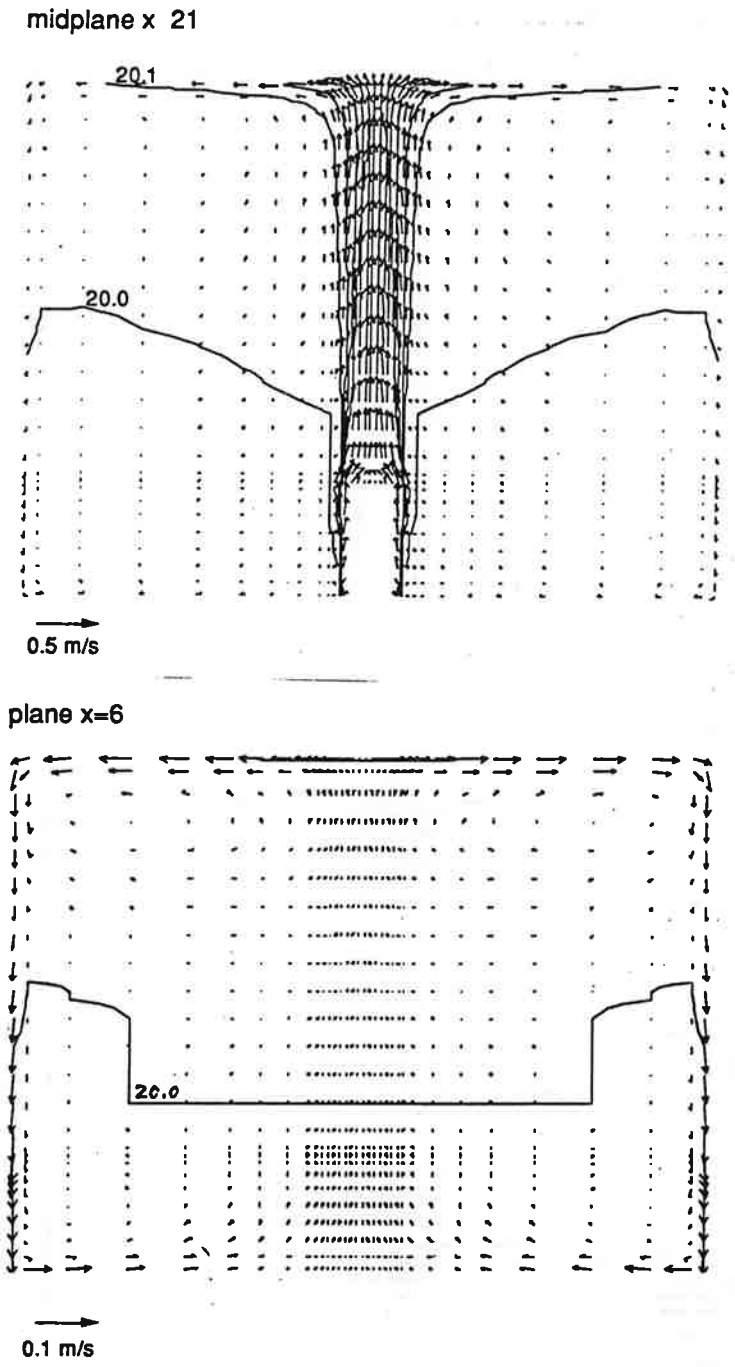

Figure 9: Case RVC21. Flow pattern and temperature contour lines in two parallel planes (see Figure 3). a) Plane x = 21 (midplane). b) Plane x = 6.

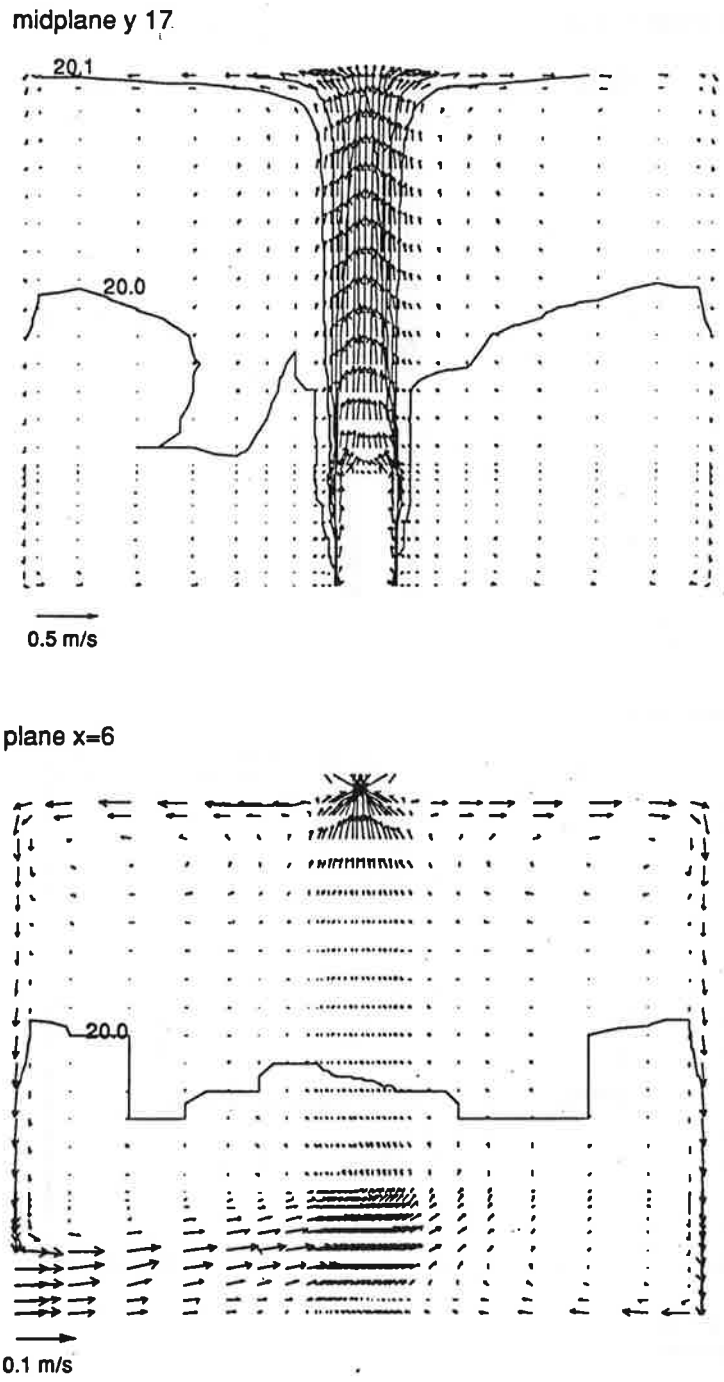

Figure 10: Case RVC92. Flow pattern and temperature contour lines in two parallel planes (see Figure 3). a) Plane x = 21 (midplane). b) Plane x = 6.

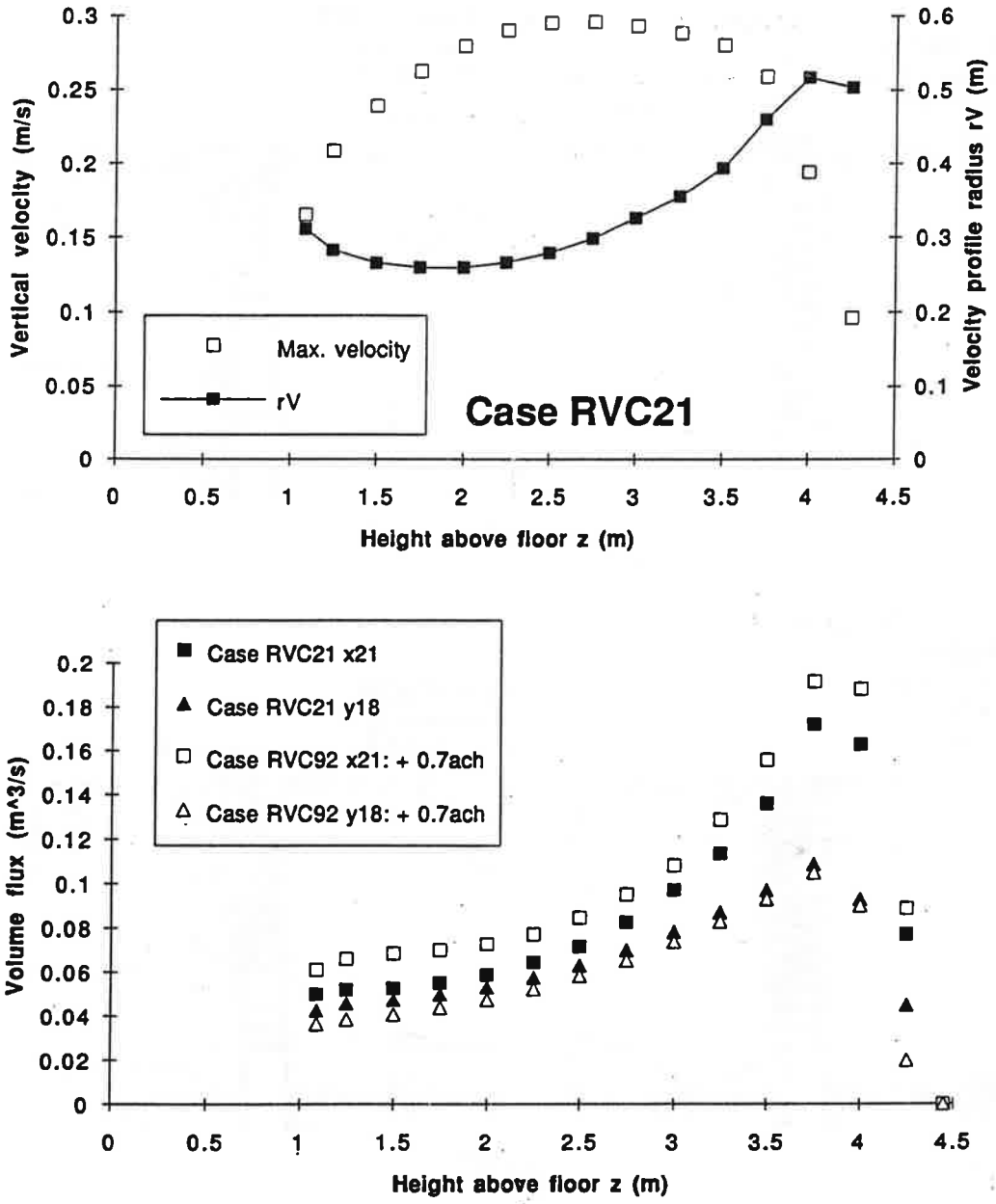

Figure 11: a) Case RVC21: Plume velocity profile maximum and radius as functions of height. b) Volume flux derived from the elocity profiles in two perpendicular planes for cases RVC21 (no ventilation) and RVC92 (ventilation rate 0.7 ach).

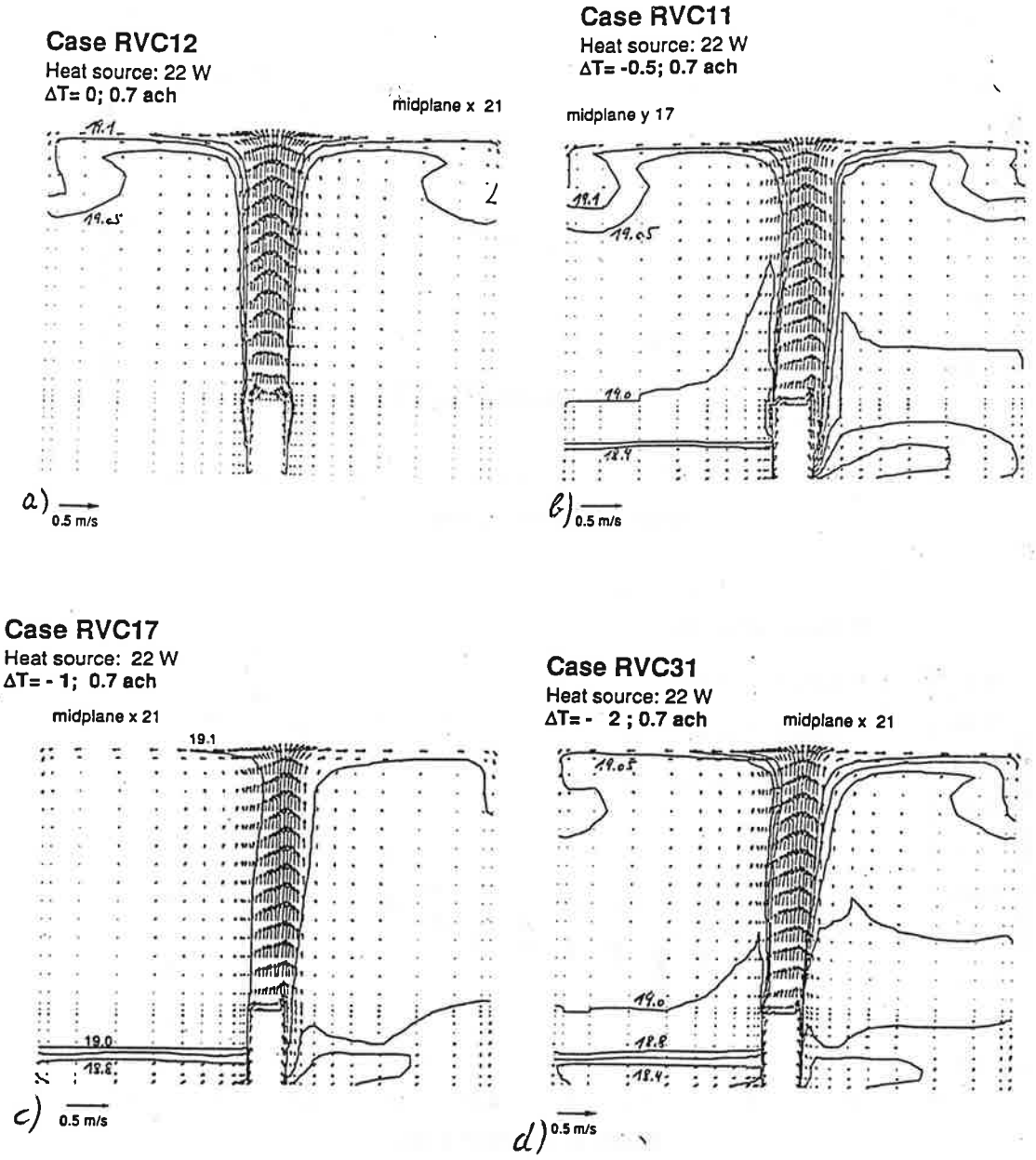

Figure 12: Comparison of flow pattern and temperature stratification in the midplane x=21 for cases with a ventilation rate of 0.7 ach. a) Case RVC12: ΔT=0 K. b) Case RVC11: ΔT= - 0.5 K. c) Case RVC17: ΔT= - 1 K. d) Case RVC31: ΔT= - 2 K.

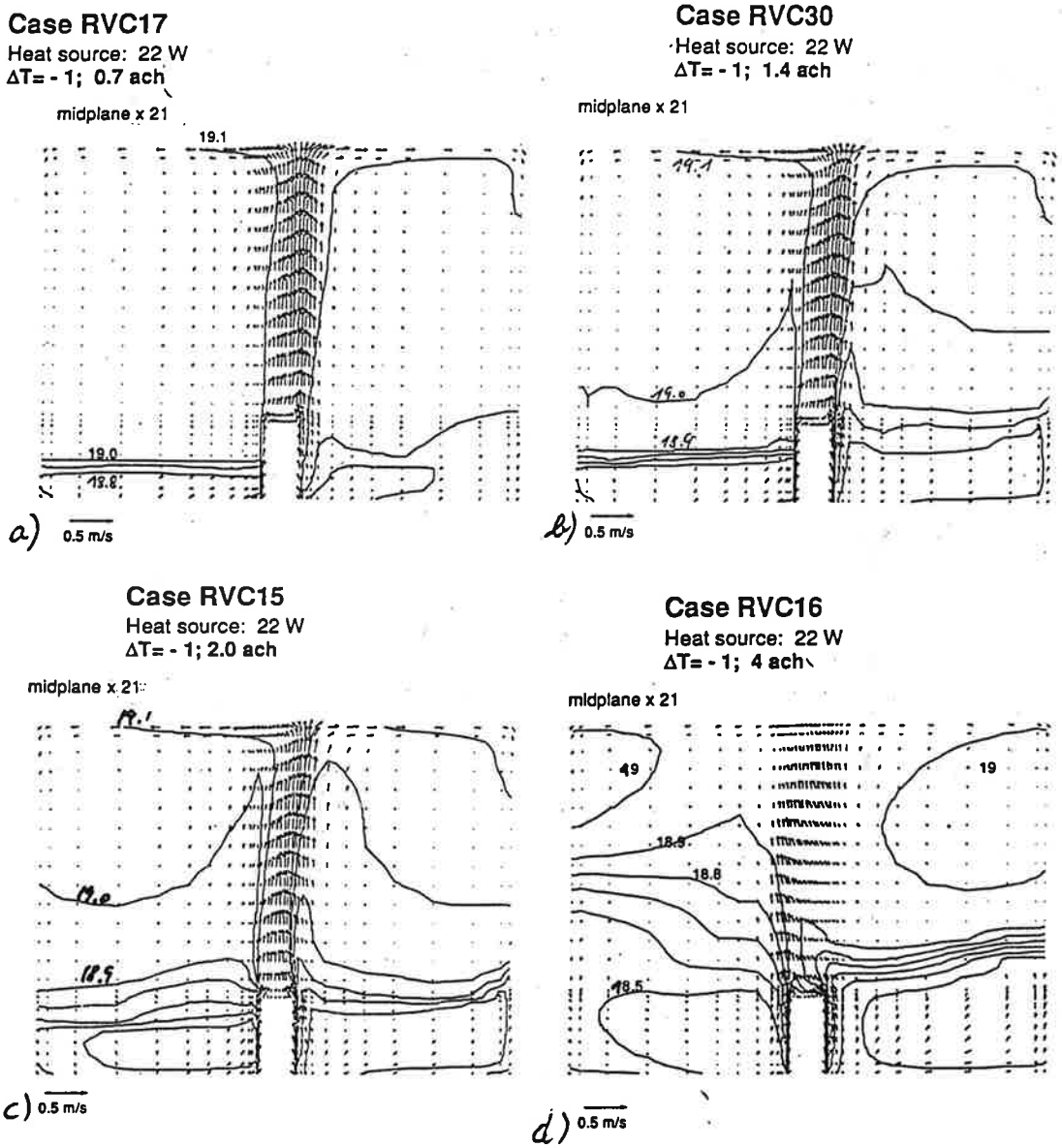

Figure 13: Comparison of flow pattern and temperature stratification in the midplane x=21 for cases with a inlet air temperature difference of -1 K. a) Case RVC17: Ventilation rate r = 0.7 ach. b) Case RVC30: r = 1.4 ach. c) Case RVC15: r = 2.0 ach. d) Case RVC16: r = 4.0 ach.